

A Fuzzy-C-Means Clustering Algorithm for a Volumetric Analysis of Paranasal Sinus and Nasal Cavity Cancers

K. Passera, P. Potepan, E. Setti, D. Vergnaghi, A. Sarti, L. Mainardi and S. Cerutti

Abstract— In this paper, a semi-automatic segmentation algorithm for volumetric analysis of paranasal sinus and nasal cavity cancers is presented and validated. The algorithm, based on a semi-supervised Fuzzy-C-means method, was applied to a Magnetic Resonance data sets (each of them composed by T1-weighted, Contrast Enhanced T1-weighted and T2-weighted images) for a total of 64 tumor-contained slices. Method performances are tested by both a numerical and a clinical validation. Results show that the proposed method has a higher accuracy in quantifying lesion area than a Region Growing algorithm and it can be applied in the evaluation of tumor response to therapy.

I. INTRODUCTION

PARANASAL sinus and nasal cavity cancers are pathologies that, after a radiotherapy treatment, may present a highly infiltrative growth pattern. In general the tumor volume cannot be easily assessed, because its irregular shape makes crude measurement difficult and limited in accuracy [1]. Often, clinicians must manually trace lesion outlines and this entails a lot of time.

Literature shows a lack of quantitative methods for paranasal sinus and nasal cavity cancers volume analysis using Magnetic Resonance Imaging (MRI) principally for the following reasons [1][2][3][4]: (1) the infiltrative growth pattern and irregular shape of tumor, (2) the complexity of neighbor anatomical tissues, usually with similar pixel intensity distribution, (3) tumor pixel intensity is often inhomogeneous, (4) partial volume effect makes lesion outlines blurred.

Classical algorithms [2] used for medical images segmentation are based on thresholding, clustering, region growing and contour extraction. Among these, clustering is the most suitable technique for our purposes, because it

permits to combine information from a set of different images even if outlines are not well-visible [2][4]. In particular, a Fuzzy approach [4][5] may take into account the uncertainty in attributing a pixel to a given class of tissue.

Bear in mind these facts, we implemented a semi-automatic method to segment paranasal sinus and nasal cavity cancers for volume analysis. Information for the segmentation process is obtained through a weighted composition of three different MR images (T1-weighted, Contrast Enhanced T1-weighted and T2-weighted images) and segmentation is based on a supervised Fuzzy-C-means (SFCM) algorithm.

The method was tested on 64 tumor-contained slices through two types of validation: i) a numerical validation in which segmentation outcomes obtained by SFCM were compared with manual segmentation performed by an experienced radiologist and ii) a more qualitative validation in which clinician criteria (including the erroneous involvement of essential anatomical structures) were considered. A comparison with Region Growing based algorithm [5] was carried out.

II. MATERIALS AND METHODS

A. Experimental Protocol and Image Acquisition

The algorithm was tested in an experimental protocol developed at the Department of Images for Diagnosis and Therapy of the National Cancer Institute of Milan. We analysed 6 patients for a total of 10 exams. All patients underwent 1.5 T MR imaging (Siemens Vision, Erlangen). Spin-echo and turbo-spin-echo sequences were used to obtain T1-weighted (T1), contrast-enhanced T1-weighted (Gadolinium, Gd-T1), T2-weighted (T2) images. The 512X512 pixel images of the head in the axial plane were acquired with a 4096 (12 bits) greyscale, slice number of 18-21, slice thickness of 5 mm and slice gap of 1 mm. A total number of 64 tumor-contained slices were considered..

B. Semi-supervised fuzzy-C-method

Semi-supervised methods use a small amount of labeled data as a guide to unsupervised techniques. This may be useful especially in difficult and noisy tasks where little a

K. Passera is with the Dipartimento di Ingegneria Biomedica, Politecnico di Milano, Italy (phone: +39-02-2399-3374; fax: +39-02-2399-3360; e-mail: katia.passera@polimi.it).

P. Potepan and D.Vergnaghi are with the Dipartimento di Diagnostica per Immagini e Radioterapia, Istituto Nazionale per la Cura e la Prevenzione dei tumori di Milano, Italy.

A. Sarti is with the Dipartimento di Elettronica e Informazione, Politecnico di Milano, Italy.

E. Setti is with Laboratorio di Analisi Radiologica Avanzata (LARA), Milan, Italy.

L. Mainardi and S. Cerutti are with the Dipartimento di Ingegneria Biomedica, Politecnico di Milano, Italy.

priori information is available, such as for brain tumor segmentation [4]. In our approach the a priori information is obtained through an automatic clusters initialization and through a selection (made by the radiologist) of a few seed pixels belonging to tumor.

Let n be the number of pixels of a slice containing tumor, $X = \{x_1, \dots, x_n\}$ is the set of the MR image data, where $x_k = (\omega_{T1}x_{T1}, \omega_{Gd-T1}x_{Gd-T1}, \omega_{T2}x_{T2})$, and where $1 \leq k \leq n$, ω_{T1} , ω_{Gd-T1} , ω_{T2} are factors weighting the contribute of T1-weighted, Contrast Enhanced T1-weighted and T2-weighted image in the clustering procedure, respectively. Let C be the image clusters number, for each data, a “fuzzy” membership [6][7], $u(x_k) = [u_{1k}, u_{2k}, \dots, u_{ck}]$ is computed. Each u_{ik} ($1 \leq i \leq C$), has a value between 0 and 1, and $\sum_{i=1}^C u_{ik} = 1$. A

matrix U , consisting of $C \times n$ elements, is defined by combining the $u(x_k)$ of each pixel.

The inclusion of a priori knowledge of known membership is obtained by partitioning the X data matrix in this way:

$$X = [X^l | X^u]$$

where X^l is the labeled and X^u is the unlabeled part of the data, respectively. Accordingly, the initial U matrix is formed by n_l columns of labeled pixel vectors having crisp membership (1 or 0) and $n - n_l$ columns of unlabeled pixel vectors whose values must be determined.

To find the values of unlabeled columns of the U matrix the following function is minimized [4]:

$$J_m = \sum_{i=1}^C \sum_{k=1}^N u_{ik}^m \|X_k - V_i\|^2, 1 \leq m \leq \infty$$

where $V_i = \{V_1, \dots, V_C\}$ are the cluster centers and m is the fuzzyfication coefficient. Let $m=2$, the objective function leads to the minimal square errors of the estimated membership matrix [5].

The first time the V_i are defined considering only the X^l data, while for the u_{ik} updating only X^u are taking into account.

The process ends when the error (distance between the new and old unlabeled columns of the U matrices) is smaller than a threshold or after a maximum number of iterations.

For our application, different settings (i.e. number of clusters and different combination of image features) were evaluated. The optimal selection algorithm of parameters was obtained using 8 clusters and setting $\omega_{T1}=0.5$, $\omega_{Gd-T1}=1$, $\omega_{T2}=0.1$.

C. Segmentation algorithm

The segmentation procedure is shown in Fig. 1. It is applied for any slice containing a tumor.

First of all, the radiologist selects one or more (if inhomogeneous) pixels belonging to tumor tissues. This is important for the successive selection of the Region of Interest (ROI) containing tumor.

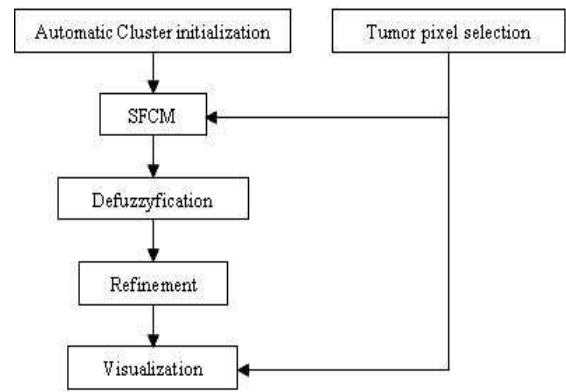


Fig. 1. Steps of segmentation algorithm

Next, the initial guess for SFCM algorithm is obtained by an automatic clusters initialization. This is realized considering the bidimensional histogram formed by T1-weighted and Contrast Enhanced T1-weighted images (Fig. 2). In this histogram the different tissues (air, spinal cord, normal tissues, mucosa and soft palate, tumor, fat) are mapped in different histogram areas where there are local maxima. Cluster centers are initialized by local maxima intensity values in the selected areas. The “tumor cluster” is initialized directly by the radiologist.

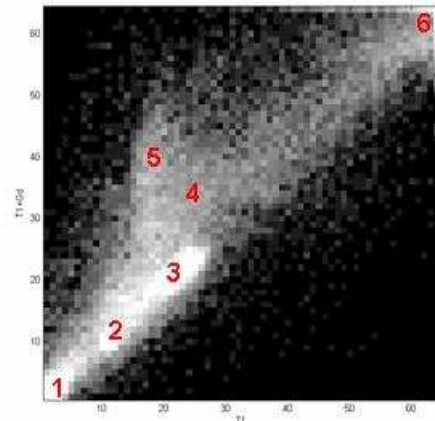


Fig. 2. T1 and T1+Gd pixels intensity distribution. Primary tissues are: (1) air, (2) spinal cord, (3) normal tissues, (4) mucosa and soft palate, (5) tumor, (6) fat.

When SFCM ends, the defuzzification operation permits to assign a label to any image pixel. Then, the segmented tumor is refined using erosion and dilatation operations in order to obtain a more accurate lesion mask [4]. Finally, the mask is superimposed on the image (see Fig. 4).

D. Validation procedure

For evaluating algorithm performances two types of validation were used. First, a numerical validation was used to compare our algorithm with a Region Growing algorithm and to quantify accuracy of the segmentation method. Then, a qualitative validation was used to evaluate the clinical usefulness of the our method.

Numerical validation.

An experienced radiologist manually segmented all 64 tumors contained in our dataset (Ground Truth, GT). Two indices were calculated [4]:

- percent match: $PM[\%] = \frac{TP}{GT} \cdot 100$;
- positive prediction value: $P+[\%] = \frac{TP}{TP + 0,5 \cdot FP} \cdot 100$;

where TP=true positives and FP=false positives. (See Fig. 3 for definition of TP and FP).

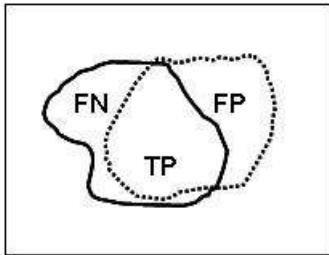


Fig. 3. Correspondence model between tumor segmented by the experienced radiologist, i.e. GT (solid line) and by the algorithm (dot line). It can be noted that $GT=TP+FN$.

PM index shows the correspondence between GT and algorithm segmentation. An ideal PM value is 100%, that is algorithm localizes perfectly tumor pixels. Conversely, the P+ index estimates the correspondence in size and location between the algorithm segmentation and GT. The 0.5 coefficient for false positives (i.e. pixels considered tumor by the algorithm, but not by GT) is introduced for taking into account that, for treatment purposes, the immediate area around tumor will also be treated and a certain degree of FP is usually acceptable.

Clinical validation

An experienced radiologist scored FCM and RG segmented tumor on the basis of three criteria:

- (1) no involvement of essential anatomical structures (i.e. optic nerve) in the tumor area.
- (2) no volume errors (underestimation or overestimation)

that may lead to errors in treatment planning.

(3) correspondence with GT.

For each segmented tumor, the radiologist checked which criteria were satisfied.

III. RESULTS

The algorithm was compared with a Region Growing (RG) algorithm [5].

An example of segmentation obtained by the two methods is shown in Fig. 4, where tumor masks were positioned on the T1-Gd image. In the original T1-Gd image, it can be noted the tumor infiltrations and the similarity of grey-levels between tumor pixels and the neighbours ones. In this case, both SFCM and RG seem to show a good performance, but using RG, a GT underestimation is present.

Table 1 reported a comparison of PM and P+ values in the case of RG, SFCM using only two images (T1-w and T1) without weighted factors as in [4] (SFCM2) and our algorithm (SFCM):

	RG	SFCM2	SFCM
PM(%)	66.26	74.09	74.65
P+(%)	82.01	81.21	89.89

We may observe that both PM and P+ increase using SFCM algorithm. In particular, P+ value indicates that our algorithm is able to correctly estimate tumor size and location.

Table 2 shows the percentage of analyzed cases in which results satisfied the clinical criteria.

Even if the three clinical criteria were better followed by SFCM, there is still the possibility to erroneously attribute important anatomical structures to tumor area.

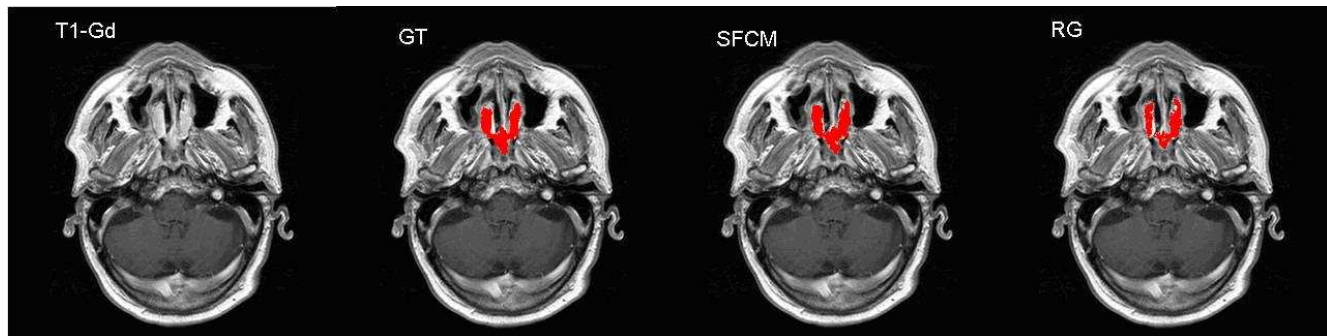


Fig. 4. Comparison between SFCM and RG outcomes with respect to GT. Masks (in red) are overlapped on the T1-Gd original image (at left).

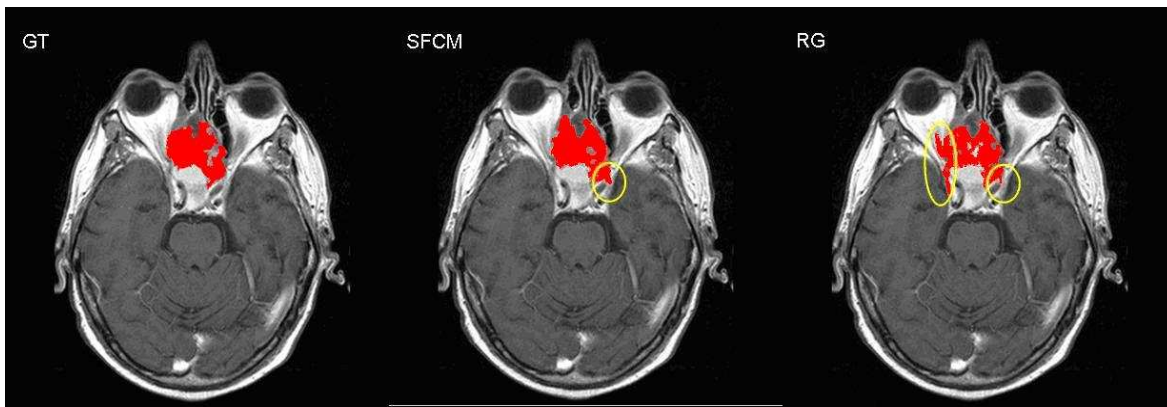


Fig. 5: Comparison between SFCM and RG outcomes with respect to GT. Both SFCM and RG present an involvement of optic nerve (yellow circled).

Table 2

	Criterion 1	Criterion 2	Criterion 3
SFCM	84,4%	89,1%	79,7%
Region Growing	59,4%	68,8%	53,1%

In Fig. 5 an example of erroneous involvement of essential anatomical structures is presented. It can be noted that, in both methods, the optical nerve is included. However, in this case the error is prominent using RG, in fact two optical nerves are included and the true tumor volume is underestimated.

IV. DISCUSSION AND CONCLUSION

The aim of this work is to develop a semi-automatic method for paranasal sinus and nasal cavity cancers segmentation and to compare its performances with those obtained by manual segmentation. The regression of paranasal sinus and nasal cavity cancers after radiotherapy treatment leads to a very irregular tumor shape. Therefore, in order to quantify the tumor regression after therapy, manual segmentation is usually performed. In literature, there are no segmentation algorithms dedicated to this pathology, conversely there are a series of articles concerning the nasopharyngeal carcinoma [1][4].

As in [4], we developed a semi-automatic clustering method based on a semi-supervised Fuzzy-C-means (SFCM) algorithm. However, in our approach, the dataset was composed by three type of MR images (T1-weighted, Contrast Enhanced T1-weighted and T2-weighted) instead of the two (T1-weighted, Contrast Enhanced T1-weighted) used by [4]. In addition, a weighting factor was introduced to balance the contribute of each image to the segmentation process. In this way, the method is more flexible and it may better mimic the segmentation process performed by clinician eyes.

In this work, our method was compared to Region Growing: both numerical results and clinical validation

show the better performance of our method, which appears to be enough accurate to evaluate the tumor response to therapy [8]. For other applications in which a more high accuracy is requested, such as radiotherapy and surgery treatment planning, the use of this method is not yet advisable.

REFERENCES

- [1] D.T.T. Chua, J.S.T Sham, D.L.W. Kwong, K.S.Tai, et al. – *Volumetric analysis of tumor extent in nasopharyngeal carcinoma and correlation with treatment outcome* – Int. J. Radiation Oncology Biol. Phys, vol.39, n°3 – 1997 – pp. 711:719.
- [2] L.P. Clarcke, R.P. Velthuisen, M.A. Camacho, et al. – *MRI segmentation: methods and applications* – Magn. Reson. Imag. 13 – 1995 – pp. 343:368.
- [3] M.Vaidyanathan, R.P. Velthuisen, P. Venugopal, L.P. Clarcke, L.O. Hall – *Tumor volume measurements using supervised and semi-supervised MRI segmentation methods* – Proceedings of the Artificial Neural Networks in Engineering, ANNIE – 1994 – pp. 629:637.
- [4] J. Zhou, T.K. Lim, V. Chong, J. Huang – *Segmentation and visualization of nasopharyngeal carcinoma using MRI* – Computers in Biology and Medicine 33 – 2003 – pp. 407:424.
- [5] W.K. Pratt – *Digital image processing: PIKS inside, Third Edition* – John Wiley & Sons, Inc. – 2001 – pp. 551:583.
- [6] R. Krishnapuram, J. Keller – *A possibilistic approach to clustering* – IEEE Trans. Fuzzy Syst. – 1993 – pp. 98:110.
- [7] R. De la Paz – *Approximate fuzzy C-means cluster analysis of medical MR images data* – IEEE Trans. GRS – 1986.
- [8] M. Vaidyanathan – *Monitoring brain tumor response to therapy using MRI segmentation* – Magnetic Resonance Imaging – 1997.